Original Article

# The Potential Protective Role of Flaxseed Oil on the Cerebellar Cortex in a Rat Model of D-Galactose-Induced Aging: Histological and Immunohistochemical Study

*Dalia El-Sayed El-Ghazouly*

*Department of Histology, Faculty of Medicine, Menoufia University, Egypt*

## ABSTRACT

**Introduction:** Aging is a natural process which affects various body's organs. Animal aging models are usually created using D-galactose (D-gal). Flaxseed oil (FSO) is nutritional supplement filled with omega-3 polyunsaturated fatty acids that have many health benefits.

**Aim of the Work:** The goal of this work was to explore the possible protective impact of flaxseed oil on the cerebellar cortex in a rat model of D-gal-induced aging.

**Materials and Methods:** Forty adult male albino rats were equally classified into four groups: Group I (Control), group II (FSO): Received flaxseed oil 1.2 ml/kg/day, group III (D-gal): Received D-galactose 200 mg/kg/day, group IV (D-gal + FSO): Received flaxseed oil and D-galactose using the identical dosages as earlier groups. For six weeks, the medication was administered once daily. At the end of this experiment, cerebellum samples were collected and provided for microscopic analysis under both light and electron microscopes. Studies using morphometrics and statistics were conducted.

**Results:** D-galactose treated group revealed severe alterations in cerebellar cortex. Molecular layer exhibited pyknotic nuclei and vacuolated neuropil. Purkinje cells appeared shrunken, irregularly shaped with shrunken heterochromatic nucleus and dilated rough endoplasmic reticulum. Many Purkinje cells were lost leaving empty spaces. Granule cells seemed to be shrunken, darkly stained and clumped in groups. Highly Significant rise in GFAP, caspase-3 and highly Significant decline in calbindin immunoreactivity relative to control group were also noticed. Highly significant changes in serum malondialdehyde and superoxide dismutase levels relative to control group were detected. Flaxseed oil administration with D-galactose minimized these changes.

**Conclusion:** Flaxseed oil can provide neuroprotective impact in the aging process through its antioxidant and anti-inflammatory effects.

**Received:** 03 June 2024, **Accepted:** 13 August 2024

**Key Words:** Aging, cerebellar cortex, d-galactose, flaxseed oil, GFAP.

**Corresponding Author:** Dalia El-Sayed El-Ghazouly, MD, Department of Histology, Faculty of Medicine, Menoufia University, Egypt, **Tel.**: +20 10 1071 1153, **E-mail:** daliaelghazouly@yahoo.com

**ISSN:** 1110-0559, Vol. 48, No. 3

## INTRODUCTION

Aging is an intricate natural process whose hallmark is degenerative alterations in cell and tissue structure[1]. It is manifested by a steady decline in physiological processes that raises the risk of illness and mortality[2]. Oxidative stress is the primary cause of aging and can result in a multitude of disorders linked to it due to cumulation of reactive oxygen species (ROS) and reduced capability of antioxidants[3].

It is projected that the number of people over 65 would surpass 800 million by 2025. An increase in disease and disability will be correlated with the elderly population. Consequently, one of the main challenges facing medical gerontology is understanding the pathophysiology of aging and associated disorders[4].

D-galactose has been widely used to create aging models in animals in order to explore aging properties and investigate anti-aging treatment interventions. Chronic administration of D-galactose had been known to trigger oxidative stress that can imitate aging properties[5,6]. The body naturally contains the reduced sugar D-galactose (D-gal). D-gal can also be found in foods like soy sauce and dairy products[7]. When D-gal levels are high, it promotes production of free radicals, attenuates activities of antioxidant enzymes, and hence induces oxidative stress by producing ROS. In various organs, including the kidney, muscle, and brain, oxidative damage and inflammation are important mediators of age-related changes[4].

Brain's aging is global issue because it was found to be the primary predisposing factor for major neurological illnesses, like Parkinson's and Alzheimer's diseases[8]. As people age, brain cells are subjected to greater oxidative stress and metabolic deterioration, resulting in protein buildup and DNA damage. These alterations may appear as worsened cognitive function and elevated anxiety[9]. Oxidative stress, inflammation and apoptosis of nerve cells are induced by excess D-gal[7].

*DOI: 10.21608/ejh.2024.294458.2080*

Due to its involvement in motor coordination and balance maintenance, the cerebellum is a crucial component of the brain. It may also be involved in some cognitive, emotional, and reward processes[10].

Linum usitatisimum L., or flaxseed, is harvest with many uses having beneficial effect on human health, including cardioprotective, neuroprotective, anti-diabetic, antioxidant, anti-inflammatory, and anticancer activities. Flaxseed oil, vitamins, fibers, lignans and proteins are nutritious components of flaxseed[11,12].

Flaxseed oil (FSO) or linseed oil is extracted from flaxseeds and is widely used as a dietary supplement all over the world[13]. Omega-3 polyunsaturated fatty acids (PUFAs) are abundant in this oil, making it among the most important oils due to numerous benefits of these fatty acids[14].

About 75% of the weight of flaxseed oil is made up of omega-3 PUFAs; of these, 40–60% is alpha-linolenic acid, while the remaining is oleic and linoleic acids (15% for each). Alpha-linolenic acid gives rise to docosahexanoic acid (DHA) and eicosapentanoic acid (EPA) and it may be good for your health and help manage chronic illnesses. The brain's phospholipid membranes are highly enriched in EPA and DHA, which support development of central nervous system, behavior and brain function[12].

Experimental research has demonstrated that omega-3 polyunsaturated fatty acid is implicated in numerous neurobiological processes related to neuroprotection and neurotransmission suggesting that these fatty acids could potentially avert age-associated brain deterioration[15].

Accordingly, the intention of this study was to determine the possible protective impact of flaxseed oil on cerebellar cortex in rat model of aging triggered by D-gal using histological and immunohistochemical methods.

## *Materials and Methods*

### *Materials*

### *Drugs*

D-galactose (D-gal) was obtained from Sigma-Aldrich (St. Louis, MO, United States). D-gal powder was injected subcutaneously after being dissolved in 0.9% saline. We dissolved 800 mg of D-gal in 20 ml saline to get solution containing 40 mg/ml.

Flaxseed oil (FSO) was bought at Egyptian local market. It is administrated to rats orally using gastric tube.

### *Animals*

This study utilized forty adult male albino rats weighing between 170 and 200 grams. Their normal and healthy circumstances were preserved by strict maintenance of hygiene and care. They were given free access to water and a healthy meal. Every animal procedure was carried out in compliance with instructions about responsible usage and care of laboratory animals as well as approved protocols (Approval number: 4/2024 HIST9).

### *Experimental design*

The rats were classified into 4 groups. Each group consisted of 10 rats. For six weeks, the medication was administered once daily

**Group I (control group):** Rats in this group were subdivided into subgroup Ia & subgroup Ib, each contained 5 rats:

- Subgroup Ia: Not treated during the entire duration of the experiment.
- Subgroup Ib: Received 1 ml saline 0.9 % orally by gastric tube.

**Group II (FSO group):** Received Flaxseed oil 1.2ml/kg/day[11] orally using gastric tube.

**Group III (D-gal group):** Received D-galactose 200 mg/kg/day[3] subcutaneously. Each animal received 1ml of D-gal solution.

**Group IV (D-gal + FSO group):** Received flaxseed oil 1h before D-galactose using the identical dosages as earlier groups.

### *Methods*

Blood samples were collected for biochemical analysis twenty-four hours after the final dose. Pentobarbital injections intraperitoneally (35 mg/kg)[16] were used to anesthetize the rats, after which they were killed. The cerebellum was extracted, cleaned, and split into two pieces. One piece was prepared for examination under a light microscope, while the other piece was prepared for examination under a transmission electron microscope.

**A- Biochemical study**

Serum levels of malondialdehyde (MDA) and superoxide dismutase (SOD) were estimated at clinical pathology lab of Menoufia University.

**B- Light microscopic study**

Tissue was put for 3 days in 10% neutral-buffered formalin and then underwent standard processing to produce regular paraffin blocks. Thin sections measuring 4μm were subsequently sliced and subjected to the following investigations:

1. Histological study: For usual histological analysis, Hematoxylin and eosin (H&E) stain was used[17] and to demonstrate Nissl's granules, toluidine blue stain was used[18].
2. Immunohistochemical study: Streptavidin–biotin complex technique[19] was used for detection of:
    - Glial fibrillary acidic protein (GFAP): to identify astrocytes. Utilizing anti-GFAP, a mouse monoclonal antibody (catalog number MS-1376-P0, Lab Vision Corporation laboratories, USA, CA94539). Brown coloration in cytoplasm of astrocyte and its processes indicated positive reaction.

- Caspase-3: to illustrate cell apoptosis, the anti-caspase-3 antibody (catalog number RB-1197-R7, USA, Lab Vision Thermo Fisher Scientific), a rabbit polyclonal antibody, was employed. Positive reaction appeared as cytoplasmic brown coloration.
- Calbindin (CB): to demonstrate calbindin (calcium-binding protein) in nerve cells. Using anti-calbindin antibody, a rabbit polyclonal antibody (E10340, Spring Bioscience, Pleasanton, CA, USA). Positive reaction appeared as cytoplasmic brown coloration.

**C- Transmission electron microscopic study**[20]

Tiny specimens were preserved in 2.5% glutaraldehyde and processed to be examined using JOEL (Japan) electron microscope at Tanta University's Faculty of Medicine in Electron Microscopic Unit.

### *Morphometric measurements*

1. Purkinje cell Number in sections stained by H&E at × 200 magnification.
2. Thickness of the granular layer in sections stained by H&E at × 200 magnification.
3. Percentage of area exhibiting GFAP immunoexpression in GFAP immuno-stained sections at × 400 magnification.
4. Percentage of area exhibiting caspase-3 immunoexpression in caspase-3 immuno-stained sections at × 400 magnification.
5. Percentage of area exhibiting calbindin immunoexpression in calbindin immuno-stained sections at × 400 magnification.

Digital image analysis system (Program Leica Q 500 MC; UK, Cambridge, Leica) was used to take all measurements in anatomy department of Menoufia University's faculty of medicine. Ten sections, chosen at random from five animals in every group, were utilized for the measurements.

### *Statistical analysis*

The findings of the biochemical and morphometric analyses have been statistically analyzed utilizing program SPSS, version 17 (IBM Corporation, Somars, NewYork, USA). The outcomes were displayed using the mean ± SEM. The "Tuckey" post hoc test was used after an ANOVA to compare the groups. If a comparison's *P value* was lower than 0.001, it was deemed highly significant; if it was below 0.05, it was deemed significant; if it was higher than 0.05, it was deemed non-significant[21].

## RESULTS

There were no recorded deaths during the entire duration of the experiment in the current study. Subgroups belonging to control group didn't exhibit any variations in the histological, immunohistochemical, morphometric, statistical results. So, it was referred to subgroups (Ia & Ib) as control group. As regard FSO group (II), there were no differences in any of the result outcomes relative to control group.

### *Light microscopic results*

**Histological study**

**• Haematoxylin and Eosin staining**

When examining H&E-stained sections of the control group (I), it was observed that the cerebellar cortex displayed its typical histological structure. This structure comprised three layers, namely inner granular, middle Purkinje cell and outer molecular layers. The outer molecular layer was composed primarily of fibers with tiny stellate cells and sparse basket cells. Middle Purkinje cell layer was made up one row of large pyriform shaped cells with central vesicular nucleus, noticeable nucleolus and basophilic cytoplasm. Surrounding the Purkinje cells were Bergmann astrocytes, which appeared pale. Inner granular layer was made up primarily of many small granule cells closely packed together, each with darkly stained rounded nuclei. Acidophilic areas were interspersed among the granule cells, representing glomeruli (cerebellar islands) (Figure 1). In contrast, D-gal group (III) exhibited severe alterations in the cerebellar cortex. The molecular layer exhibited pyknotic nuclei. In some areas, the molecular layer showed vacuolated neuropil (Figures 2,3,6). The Purkinje cells appeared shrunken, irregularly shaped and darkly stained with nucleus showing pyknosis. In some areas, there were empty neuropils around Purkinje cells. Remnants of Purkinje cells were noticed. There was focal loss of many Purkinje cells leaving empty spaces. In some areas, Purkinje cells were arranged in multiple layers with invasion of the molecular layer (Figures 2,3,4,5,6). Granule cells seemed to be shrunken, darkly stained and clumped in groups. There was a noticeable decline in granular layer's thickness in some areas. Granule cells seemed to be few in number, shrunken and widely separated in some places (Figures 2,3,4,6). Congested blood vessels were seen in all cerebellar cortex's layers (Figures 4,5). Sections from group IV showed high level of preservation in cerebellar cortex's histological structure. Most Purkinje cells had basophilic cytoplasm, vesicular nucleus and noticeable nucleolus. A small number of Purkinje cells seemed to be shrunken, darkly stained with pyknotic nucleus. The molecular and granular layers had normal appearance except for slightly congested blood vessels (Figure7).

**• Toluidine blue staining**

Sections stained with toluidine blue in the control group (I) displayed Purkinje cells characterized by a vesicular nucleus and a cytoplasm that was dark blue having Nissl's granules. Granule cells were more deeply stained (Figure 8). In contrast, D-gal group (III) revealed reduced stain intensity in Purkinje and granule cells (Figure 9). Sections from group IV (D-gal + FSO) exhibited most of Purkinje

cells appeared nearly normal with dark blue cytoplasm having Nissl's granules. Few cells appeared shrunken and irregular with reduced stain intensity. The granule cells were moderately stained (Figure 10).

### *Immunohistochemical study*

**Glial fibrillary acidic protein (GFAP) immunostaining**

The control group (I) revealed mild positive cytoplasmic GFAP immunoreaction in few astrocytes scattered throughout the various cerebellar cortex layers. The astrocyte appeared with few and thin processes (Figure 11). In contrast, D-gal group (III) exhibited strong positive cytoplasmic GFAP immunoreaction in many astrocytes in various Cerebellar Cortex layers. The astrocyte appeared with many and thick processes (Figure 12). Regarding group IV (D-gal + FSO), it exhibited moderate positive cytoplasmic GFAP immunoreaction in some astrocytes scattered throughout various cerebellar cortex layers. The astrocyte appeared with thin processes (Figure 13).

**Caspase-3 immunostaining**

The control group (I) demonstrated negative cytoplasmic immunoreaction for caspase-3 in cerebellar cortex's cells (Figure 14). In contrast, D-gal group (III) exhibited strong positive immunoreaction in cerebellar cortex's cells (Figure 15). While group IV (D-gal + FSO), displayed mild positive immunoreaction in cerebellar cortex's cells (Figure 16).

**Calbindin (CB) immunostaining**

Control group (I) demonstrated strong positive cytoplasmic immunoreaction for CB in Purkinje cells and moderate immunoreaction in the cells of molecular and granular layers (Figure 17). D-gal group (III) exhibited negative cytoplasmic CB immunoreaction in Purkinje cells and cells of molecular and granular layers (Figure 18). Regarding group IV (D-gal + FSO), it exhibited strong CB immunoreaction in most of Purkinje cells while few Purkinje cells appeared with negative CB immunoreaction. The cells of molecular and granular layers exhibited mild CB immunoreaction (Figure 19).

### *Transmission electron microscopic results*

The electron microscopy findings of the control group (I) showed typical ultrastructure of the different layers of cerebellar cortex. The molecular layer contained several myelinated nerve fibers of varying size and shape. The myelinated nerve fibers displayed an intact and tightly packed lamellar structure of the myelin sheath, containing mitochondria within the axoplasm (Figure 20). The Purkinje cells owned euchromatic nucleus with double walled nuclear membrane. Their cytoplasm contained Golgi apparatus, mitochondria having regular intact cristae, free ribosomes and rough endoplasmic reticulum (Figures 21,22). The granule cells possessed heterochromatic nucleus holding clumps of chromatin and surrounded by narrow cytoplasmic rim that contained mitochondria and free ribosomes. Some myelinated nerve fibers with intact tightly packed myelin sheath were noticed in granular layer (Figure 23). In contrast, D-gal group (III) exhibited remarkable ultrastructure changes involving the different layers of cerebellar cortex. In molecular layer, many myelinated nerve fibers showed irregular dilatation with a decrease in myelin thickness and rarefaction of axoplasm, other nerve fibers showed splitting and disruption in myelin sheath (Figure 24). Regarding Purkinje cell layer, some cells had electron dense nucleus and cytoplasm with ill-defined nuclear envelop showing indentation. Other Purkinje cells seemed to be shrunken with shrunken heterochromatic nucleus, dilated rough endoplasmic reticulum and dilated smooth endoplasmic reticulum. Near to Purkinje cells, some myelinated axons showed irregular dilatation with a decrease in their myelin thickness and rarefaction of their axoplasm (Figures 25,26,27). Some granule cells showed destruction of the cellular processes. Their nuclei were irregular with more condensed chromatin. Some apoptotic cells were noticed. Mitochondria with destroyed cristae were observed. Spaces were seen between the granule cells. Dilated congested blood vessels were seen in granular layer (Figures 28,29).

Interestingly, group IV (D-gal + FSO) exhibited much preservation of the ultrastructure of the cerebellar cortex. Majority of nerve fibers in molecular layer had normal structure with intact compact lamellar structure of myelin sheath. Few myelinated nerve fibers displayed loss of compact lamellar structure with splitting (Figure 30). Purkinje cells had euchromatic nucleus with double walled nuclear membrane. Their cytoplasm contained free ribosomes, cisternae of rough endoplasmic reticulum and mitochondria with regular intact cristae (Figure 31). Most granule cells appeared normal with heterochromatic nucleus and surrounded by narrow cytoplasmic rim containing mitochondria. Few granule cells had shrunken and irregular nuclei with more condensed chromatin. Most nearby myelinated nerve fibers had normal structure, but few displayed decrease in their myelin thickness and rarefaction of the axoplasm (Figure 32).

### *Statistical results*

**Biochemical results**

**1- Serum MDA Level**

Serum MDA level of group III (D-gal treated) revealed highly significant increase relative to control group. Group IV (D-gal + FSO) demonstrated significant increase in the identical measure relative to control group. Comparing group IV to group III, there was highly significant reduction in group IV. (Table 1, Histogram 1).

**2- Serum SOD Level**

Comparing serum SOD level of group III (D-gal treated) to that of control group, there was highly significant decline. Group IV (D-gal + FSO) exhibited significant reduction in the identical measure relative to control group. Comparing group IV to group III, there was highly significant rise in group IV. (Table 1, Histogram 2).

### *Morphometric results*

**1- Number of Purkinje cells**

Group III (D-gal treated) exhibited significant decline in mean number of Purkinje cells in comparison with control group. Group IV (D-gal + FSO) demonstrated non-significant decline in the identical measure relative to control group. When compared group IV to group III, there was significant rise in group IV (Table 2, Histogram 3).

**2- Thickness of the granular layer**

Group III (D-gal treated) demonstrated highly significant decline in granular layer thickness relative to control group. Group IV (D-gal + FSO) demonstrated non-significant decrease in the identical measure relative to control group. When compared group IV to group III, there was highly significant rise in group IV (Table 2, Histogram 4).

**3- Area percentage of GFAP immunoexpression**

Group III (D-gal treated) demonstrated highly significant rise in mean area percentage of GFAP immunoexpression in comparison with control. Group IV (D-gal + FSO) demonstrated significant rise in the identical measure relative to control group. When compared group IV to group III, there was highly significant decline in group IV (Table 2, Histogram 5).

**4- Area percentage of caspase-3 immunoexpression**

Group III (D-gal treated) exhibited highly significant rise in area percentage of caspase-3 immunoexpression relative to control group. Group IV (D-gal + FSO) demonstrated highly significant rise in the identical measure relative to control group. When compared group IV to group III, there was highly significant decline in group IV (Table 2, Histogram 6).

**5- Area percentage of calbindin immunoexpression**

D-gal treated group (III) exhibited highly significant reduction in mean area percentage of calbindin immunoexpression relative to control group. Group IV (D-gal + FSO) demonstrated highly significant reduction in the identical measure relative to control group. When compared group IV to group III, there was highly significant rise in group IV (Table 2, Histogram 7).

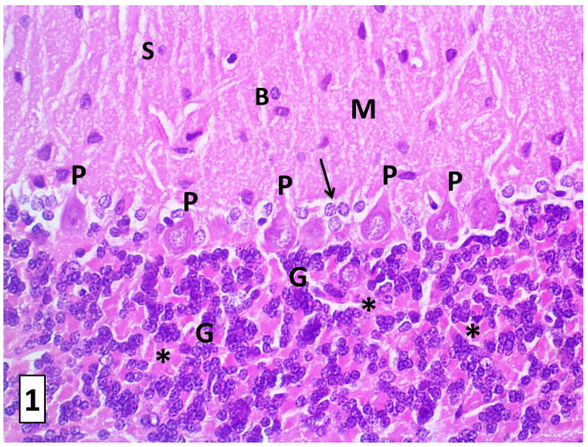


**Fig. 1:** A Photomicrograph of a section in the cerebellar cortex of the control group (I) showing its three layers. The outer molecular layer (M) is composed mainly of fibers with scattered basket cells (B) and small stellate cells (S). The middle Purkinje cell layer is formed of one row of large pyriform shaped Purkinje cells (P) with basophilic cytoplasm, central vesicular nucleus and prominent nucleolus. The inner granular layer is formed mainly of numerous small closely packed granule cells (G) having darkly stained rounded nuclei. Lightly stained acidophilic areas representing glomeruli (cerebellar islands) (*) are scattered in-between the granule cells. Notice: Bergmann astrocytes (arrows) appear pale around the Purkinje cells. (H&E × 400)

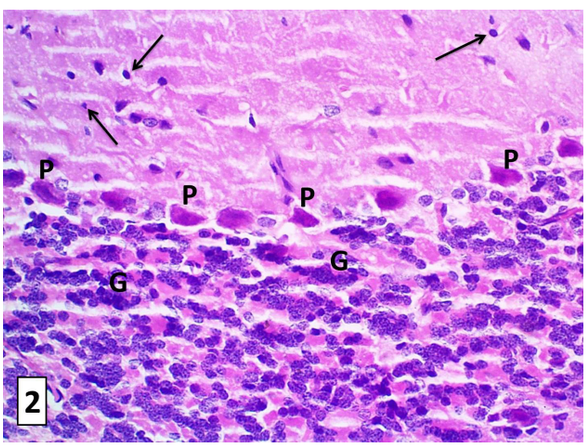


**Fig. 2:** A Photomicrograph of a section in the cerebellar cortex of D-gal group (III) showing the molecular layer with some pyknotic nuclei (arrows). The Purkinje cells (P) appear shrunken, irregularly shaped and deeply stained with pyknotic nuclei. Some granule cells appear with hyperchromatic nuclei and clumped in groups (G). (H&E × 400)

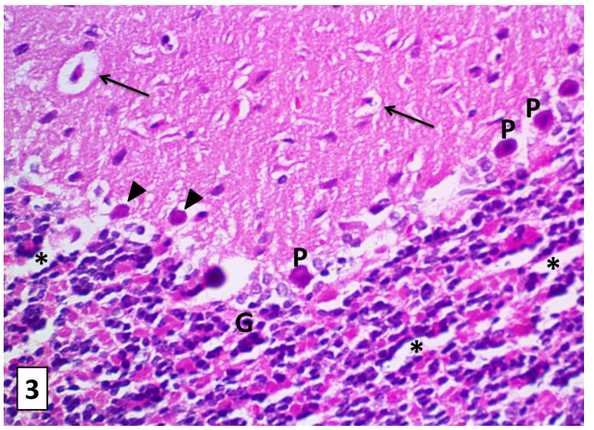


**Fig. 3:** A Photomicrograph of a section in the cerebellar cortex of D-gal group (III) showing vacuolated neuropil (arrows) in the molecular layer. The Purkinje cells (P) appear shrunken, irregularly shaped and deeply stained with pyknotic nuclei. Remnants of Purkinje cells (arrowhead) are noticed. The granule cells (G) appear shrunken, deeply stained, and clumped in groups. Notice: spaces (*) are seen in-between the granule cells. (H&E × 400)

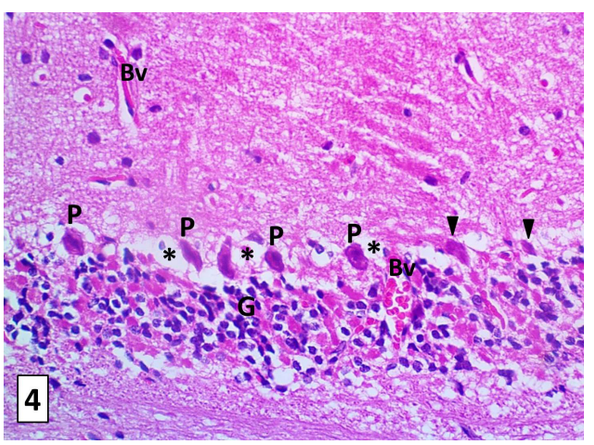


**Fig. 4:** A Photomicrograph of a section in the cerebellar cortex of D-gal group (III) showing apparent decrease in the thickness of the granular layer. The granule cells (G) appear few in number, shrunken, deeply stained and widely separated. Congested blood vessels (Bv) are seen in the molecular and granular layers. The Purkinje cells (P) appear shrunken, irregularly shaped and deeply stained with pyknotic nuclei. Remnants of Purkinje cells are noticed. Notice, the Purkinje cells are surrounded by empty neuropils (*). (H&E × 400)

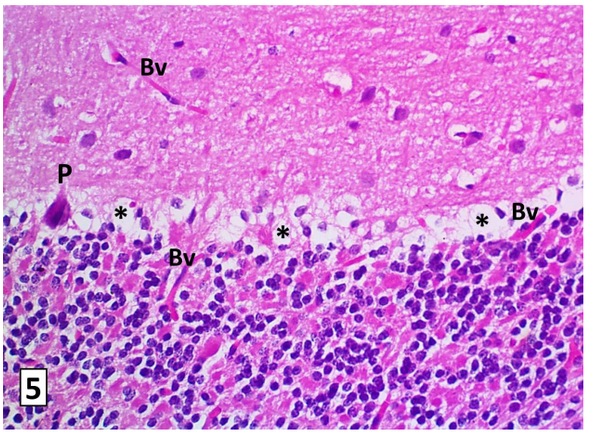


**Fig. 5:** A Photomicrograph of a section in the cerebellar cortex of D-gal group (III) showing focal loss of many of Purkinje cells leaving empty spaces (*). One Purkinje cell (P) appears shrunken with pyknotic nuclei. Congested blood vessels (Bv) are noticed in the three layers of cerebellar cortex. (H&E × 400)

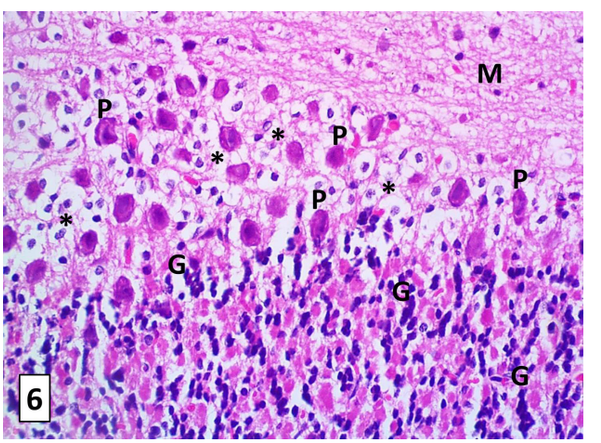


**Fig. 6:** A Photomicrograph of a section in the cerebellar cortex of D-gal group (III) showing irregularly shaped deeply stained Purkinje cells with pyknotic nuclei (P) arranged in multiple layers with invasion of the molecular layer. Purkinje cells are surrounded by vacuolated neuropil (*). The granule cells (G) appear few in number, shrunken, deeply stained, clumped and widely separated. Notice: the molecular layer (M) shows vacuolated neuropil. (H&E × 400)

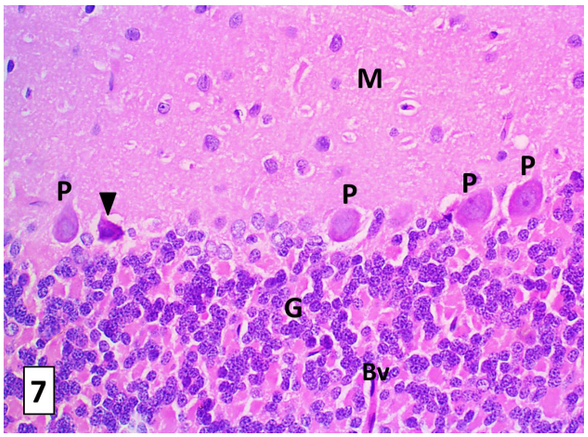


**Fig. 7:** A Photomicrograph of a section in the cerebellar cortex of D-gal + FSO group (IV) showing most of Purkinje cells (P) appearing with basophilic cytoplasm, vesicular nuclei and prominent nucleoli. One Purkinje cells (arrowhead) appear shrunken, darkly stained with pyknotic nucleus. The molecular (M) and granular (G) layers have a normal appearance. Slightly congested blood vessel (Bv) is seen in the granular layer. (H&E × 400)

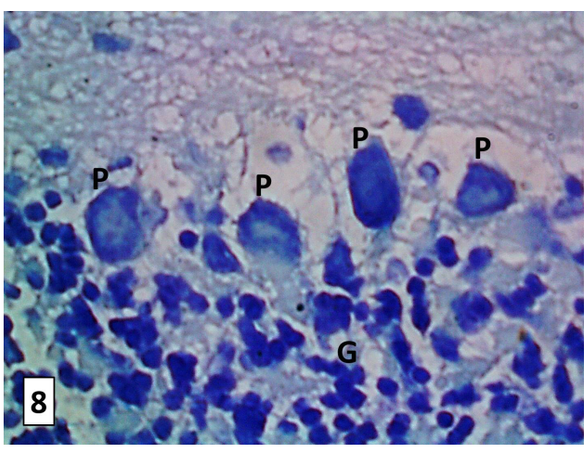


**Fig. 8:** A Photomicrograph of a section in the cerebellar cortex of the control group (I) showing flask shaped to rounded purkinje cells (P) with vesicular nucleus and dark blue cytoplasm containing Nissl's granules. The granule cells (G) are more deeply stained. (T.B. × 1000)

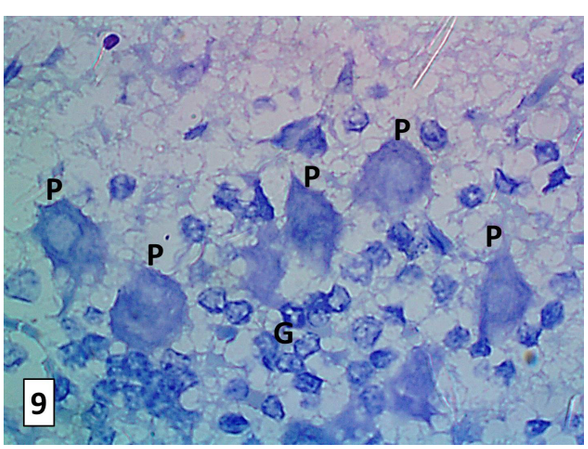


**Fig. 9:** A Photomicrograph of a section in the cerebellar cortex of D-gal group (III) showing decreased intensity of stain for Nissl's granules in the cytoplasm of Purkinje (P) and granule cells (G). (T.B. × 1000)

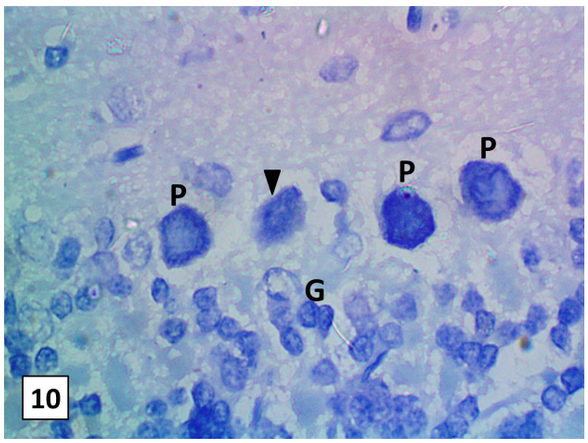


**Fig. 10:** A Photomicrograph of a section in the cerebellar cortex of D-gal + FSO group (IV) showing most of Purkinje cells (P) appear nearly normal with vesicular nucleus and dark blue cytoplasm containing Nissl's granules. One Purkinje cell (arrowhead) appears shrunken and irregular with decreased intensity of stain for Nissl's granules. The granule cells (G) are moderately stained. (T.B. × 1000)

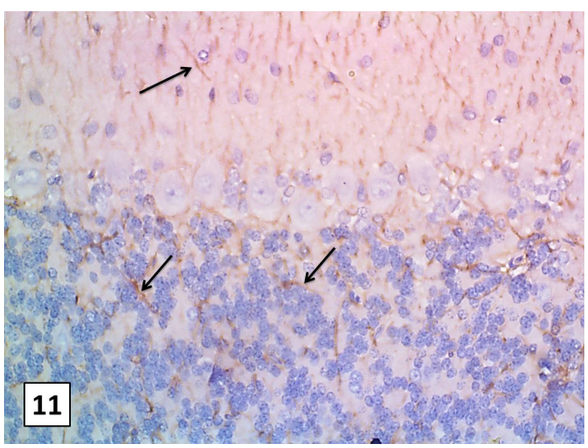


**Fig. 11:** A Photomicrograph of a section in the cerebellar cortex of the control group (I) showing mild positive cytoplasmic GFAP immunoreaction in few astrocytes (arrows) dispersed between the different layers of cerebellar cortex. Notice: the astrocytes have few and thin processes. (GFAP × 400)

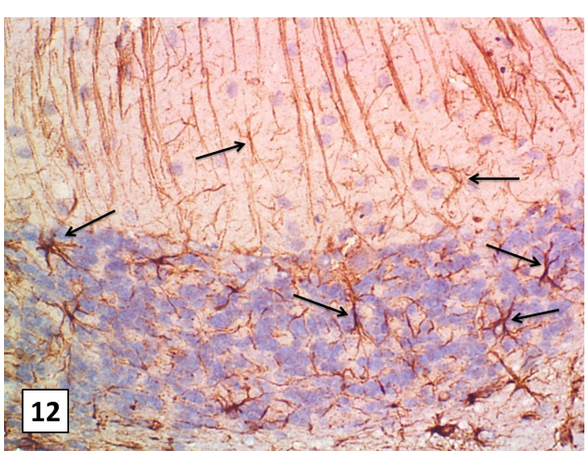


**Fig. 12:** A Photomicrograph of a section in the cerebellar cortex of D-gal group (III) showing strong positive cytoplasmic GFAP immunoreaction in many astrocytes (arrows) dispersed between the different layers of cerebellar cortex. Notice: the astrocytes have many and thick processes. (GFAP × 400)

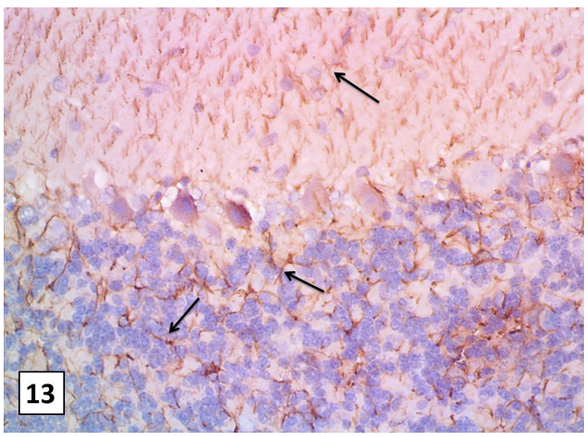


**Fig. 13:** A Photomicrograph of a section in the cerebellar cortex of D-gal + FSO group (IV) showing moderate positive cytoplasmic GFAP immunoreaction in some astrocytes (arrows) dispersed between the different layers of cerebellar cortex. Notice: the astrocytes have thin processes. (GFAP × 400)

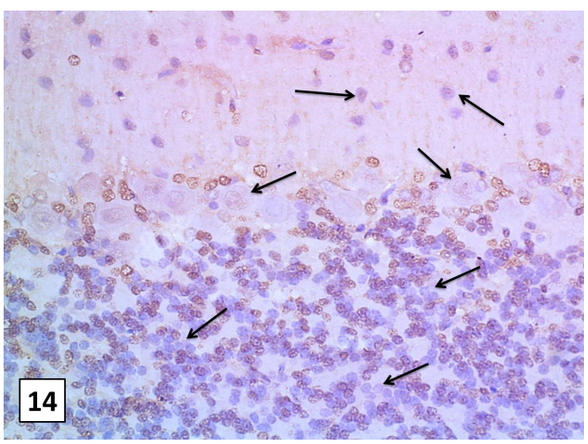


**Fig. 14:** A Photomicrograph of a section in the cerebellar cortex of the control group (I) showing negative cytoplasmic immunoreaction for caspase-3 in different cells of different layers of cerebellar cortex (arrows). (Caspase-3 X 400)

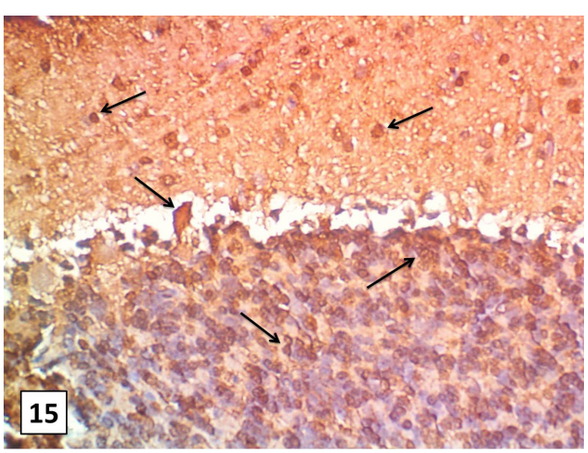


**Fig. 15:** A Photomicrograph of a section in the cerebellar cortex of D-gal group (III) showing strong positive cytoplasmic immunoreaction for caspase-3 in different cells of different layers of cerebellar cortex (arrows). (Caspase-3 × 400)

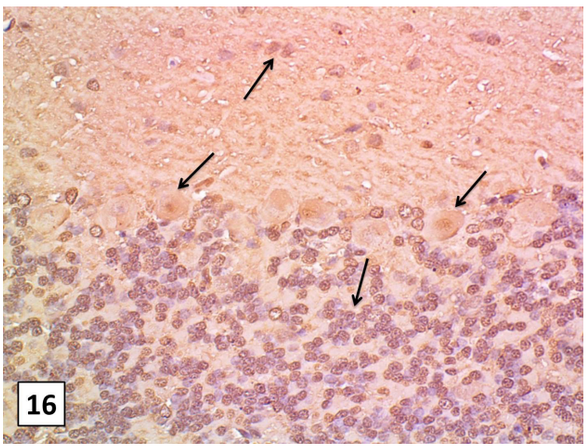


**Fig. 16:** A Photomicrograph of a section in the cerebellar cortex of D-gal + FSO group (IV) showing mild positive cytoplasmic immunoreaction for caspase-3 in different cells of different layers of cerebellar cortex. (Caspase-3 × 400)

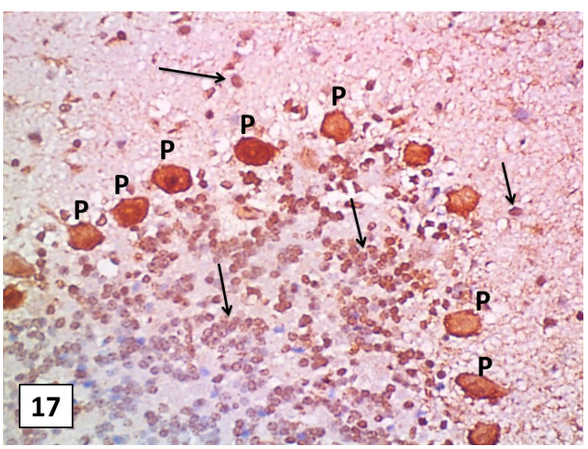


**Fig. 17:** A Photomicrograph of a section in the cerebellar cortex of the control group (I) showing strong positive cytoplasmic immunoreaction for CB in Purkinje cells (P). The cells of molecular and granular layers exhibit moderate immunoreaction for CB (arrows). (CB × 400)

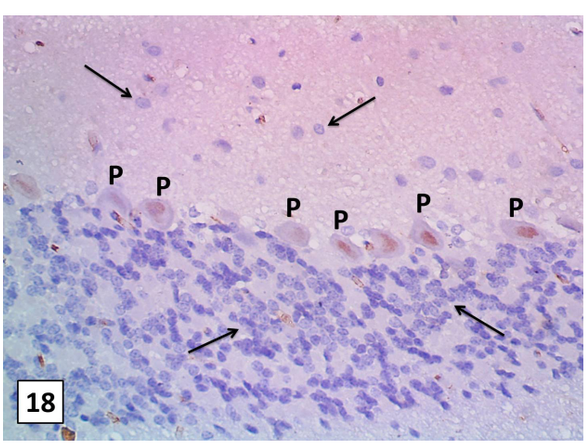


**Fig. 18:** A Photomicrograph of a section in the cerebellar cortex of D-gal group (III) showing negative cytoplasmic immunoreaction for CB in Purkinje cells (P), cells of molecular and granular layers (arrows). (CB × 400)

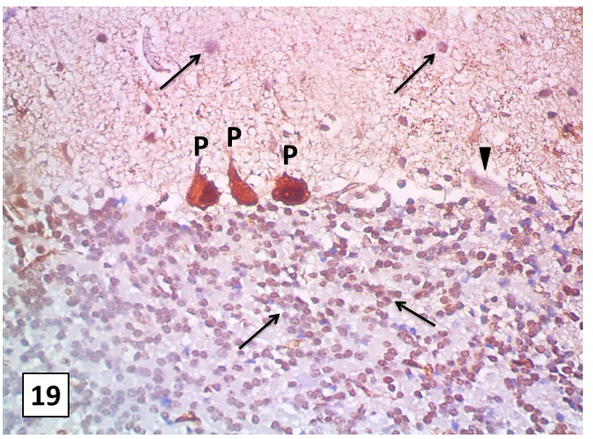


**Fig. 19:** A Photomicrograph of a section in the cerebellar cortex of D-gal + FSO group (IV) showing strong positive cytoplasmic immunoreaction for CB in most of Purkinje cells (P), one Purkinje cell appears with negative CB immunoreaction (arrowhead). The cells of molecular and granular layers exhibit mild CB immunoreaction (arrows). (CB × 400)

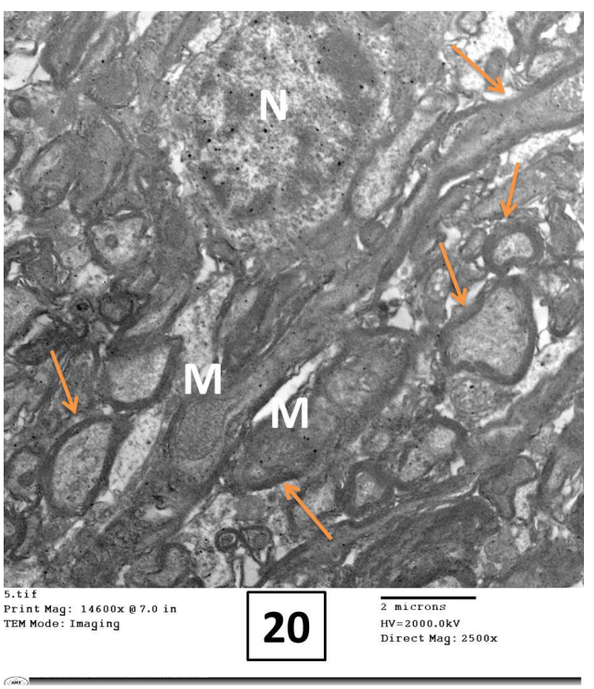


**Fig. 20:** An electron micrograph from the control group (I) showing the molecular layer of the cerebellar cortex containing several myelinated nerve fibers of varying size and shape (orange arrows). Myelinated nerve fibers reveal intact tightly packed lamellar structure of myelin sheath with mitochondria (M) in their axoplasm. A cell with heterochromatic nucleus (N) is observed among nerve fibers. (TEM × 2500)

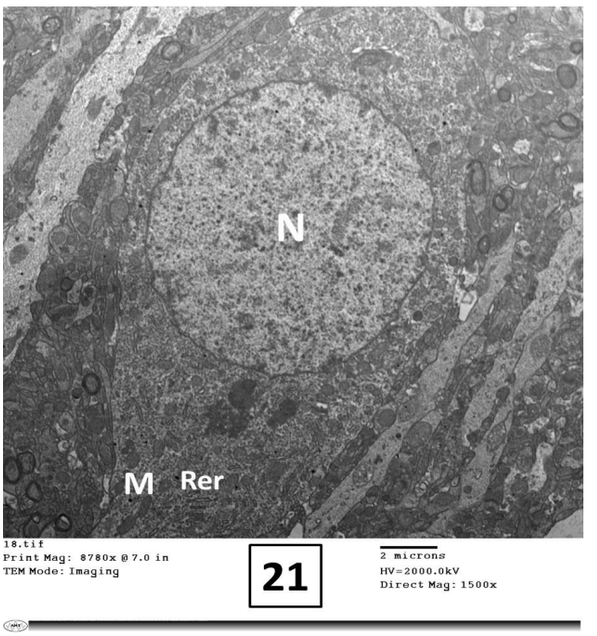


**Fig. 21:** An electron micrograph from the control group (I) showing pyriform Purkinje cell with euchromatic nucleus (N). The cytoplasm contains many mitochondria (M) and several cisternae of rough endoplasmic reticulum (Rer). (TEM × 1500)

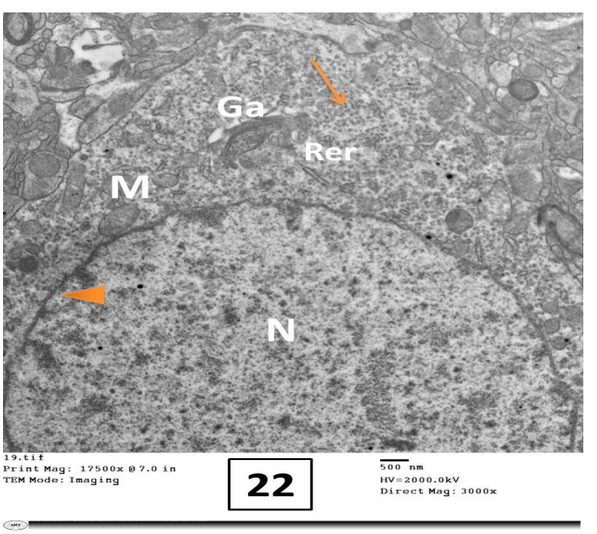


**Fig. 22:** Higher magnification of the previous section showing Purkinje cell with euchromatic nucleus (N). The nuclear membrane appeared double walled (arrowhead). The cytoplasm contains Golgi apparatus (Ga), mitochondria (M) with regular intact cristae, cisternae of rough endoplasmic reticulum (Rer) and free ribosomes (arrow). (TEM × 3000)

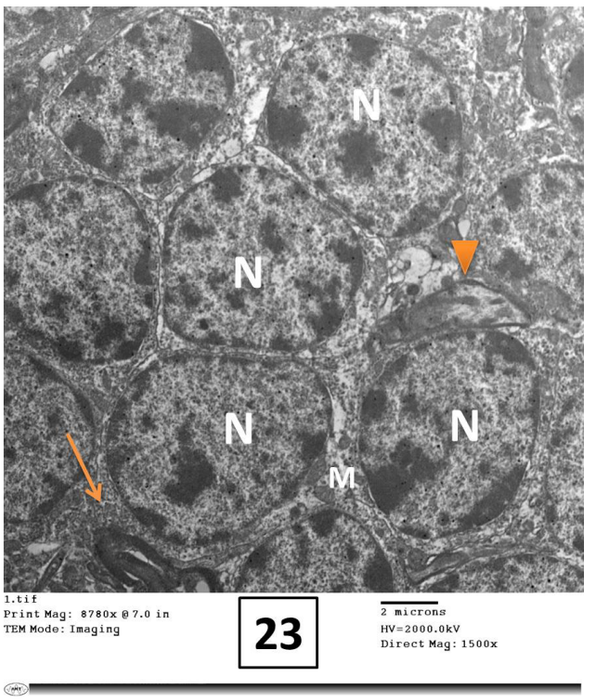


**Fig. 23:** An electron micrograph from the control group (I) showing closely packed granule cells with heterochromatic nucleus (N) containing clumps of chromatin and surrounded by thin rim of cytoplasm. Their cytoplasm contains mitochondria (M) and free ribosomes (orange arrow). Notice: A myelinated nerve fiber appears with compact myelin sheath (arrowhead). (TEM × 1500)

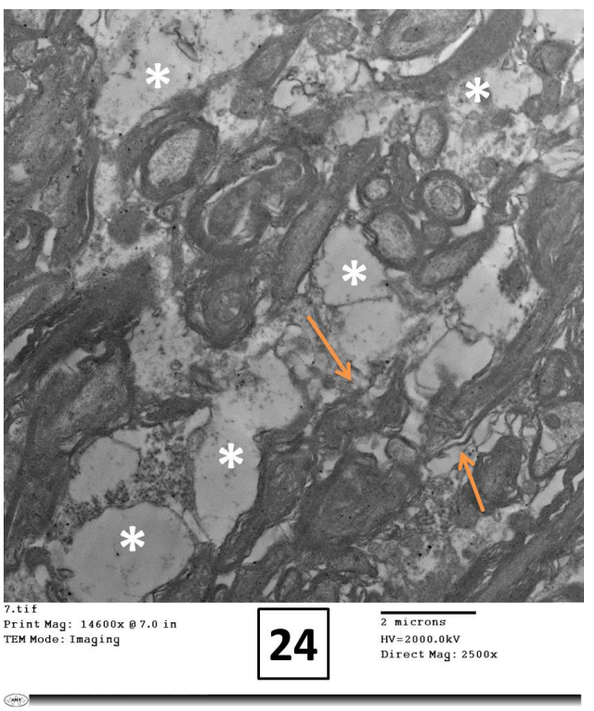


**Fig. 24:** An electron micrograph from D-gal group (III) showing many myelinated nerve fibers in the molecular layer of the cerebellar cortex appearing irregularly dilated with thinning of their myelin and rarefaction of their axoplasm (*). Some myelinated nerve fibers appear with splitting and disruption of myelin sheath (orange arrows). (TEM × 2500)

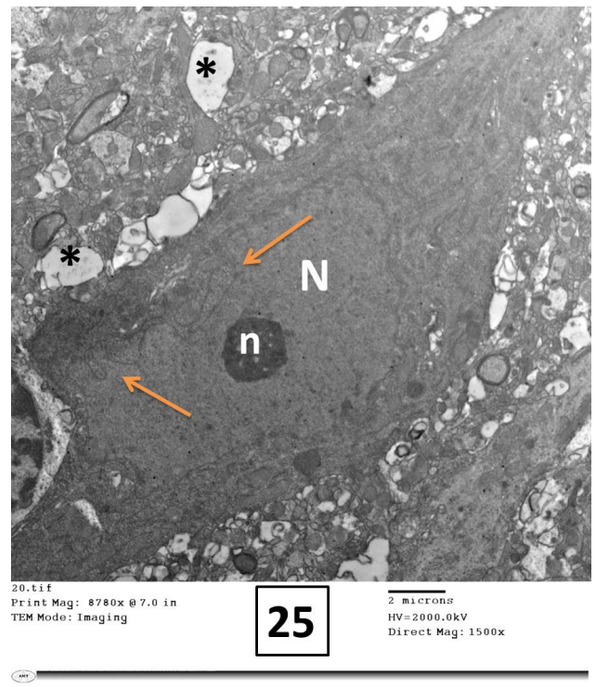


**Fig. 25:** An electron micrograph from D-gal group (III) showing irregular Purkinje cell with electron dense nucleus (N) and cytoplasm. The nucleus has prominent nucleolus (n) and ill-defined nuclear envelop showing indentation (orange arrows). Some nearby myelinated axons show rarefaction of their axoplasm (*). (TEM × 1500)

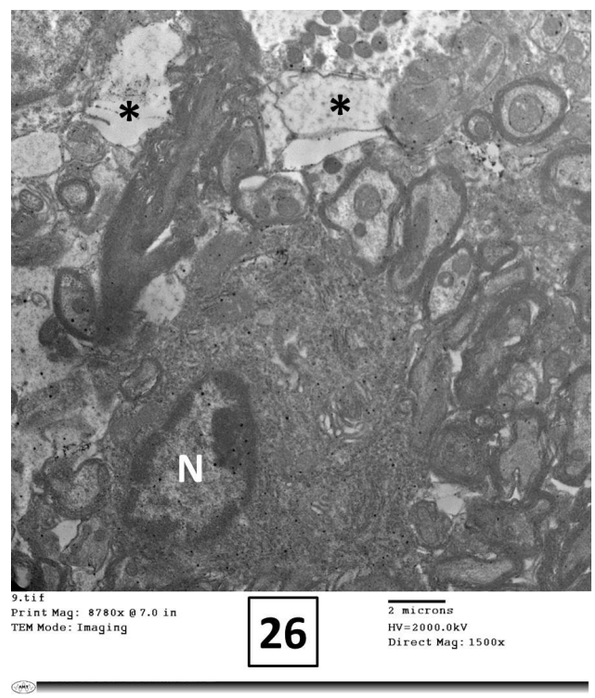


**Fig. 26:** An electron micrograph from D-gal group (III) showing shrunken Purkinje cell with shrunken heterochromatic nucleus (N). Some nearby myelinated axons are irregularly dilated with thinning of their myelin and rarefaction of their axoplasm (*). (TEM X1500)

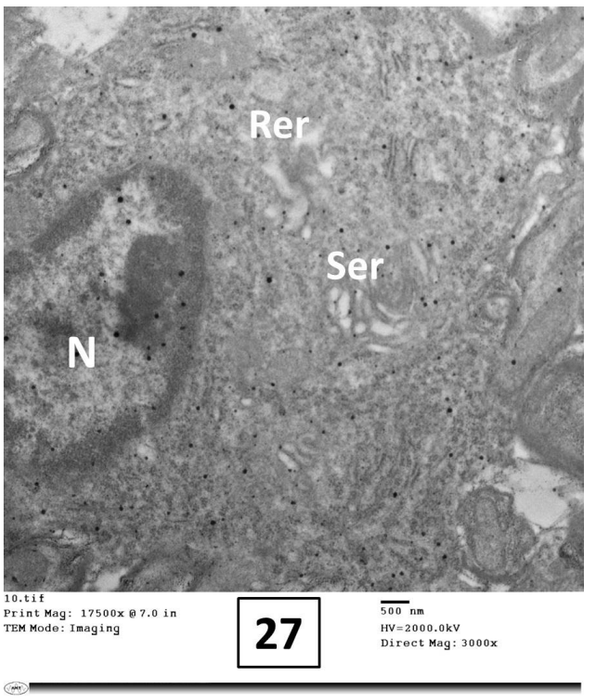


**Fig. 27:** Higher magnification of the previous section showing Purkinje cell with shrunken heterochromatic nucleus (N). The cytoplasm contains dilated rough endoplasmic reticulum (Rer) and smooth endoplasmic reticulum (Ser). (TEM × 3000)

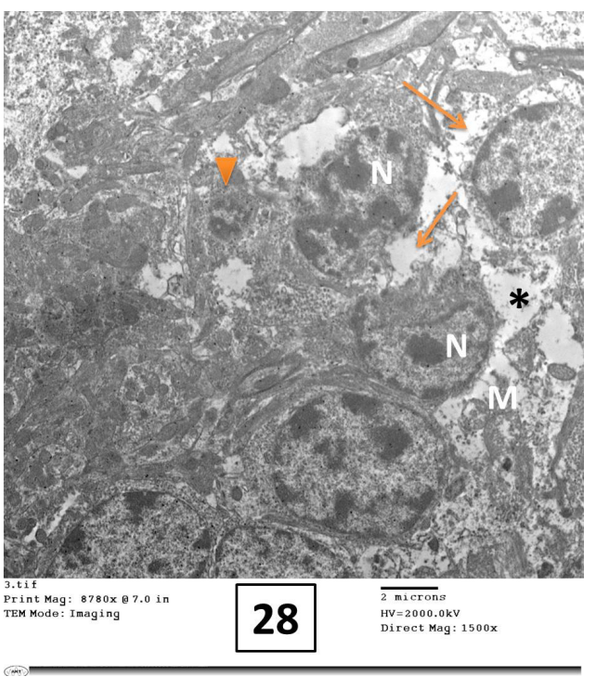


**Fig. 28:** An electron micrograph from D-gal group (III) showing destruction of the cellular processes of the granule cells (orange arrows) with one apoptotic cell (orange arrowhead). Some nuclei (N) appear irregular with more condensed chromatin. Mitochondria (M) with destroyed cristae are observed. Spaces are seen in between the cells (*). (TEM × 1500)

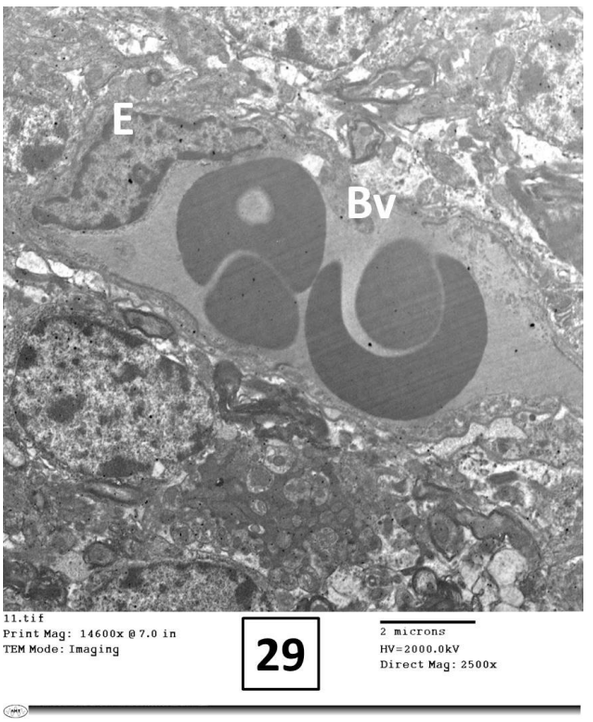


**Fig. 29:** An electron micrograph from D-gal group (III) showing dilated congested blood vessel (Bv). Notice: endothelial cell (E) lining the wall of the blood vessel. (TEM × 2500)

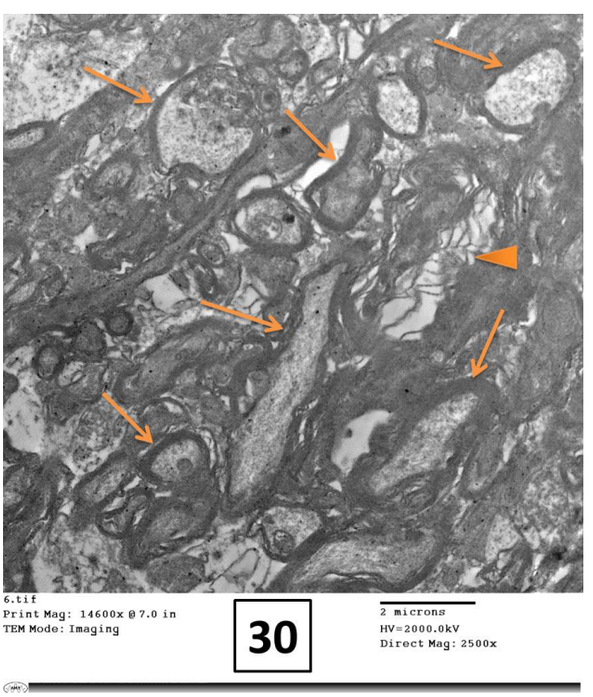


**Fig. 30:** An electron micrograph from D-gal + FSO group (IV) showing most of the myelinated nerve fibers in the molecular layer preserving their normal structure with intact compact lamellar structure of myelin sheath (orange arrows). Few myelinated nerve fibers display loss of compact lamellar structure with splitting (arrowhead). (TEM × 2500)

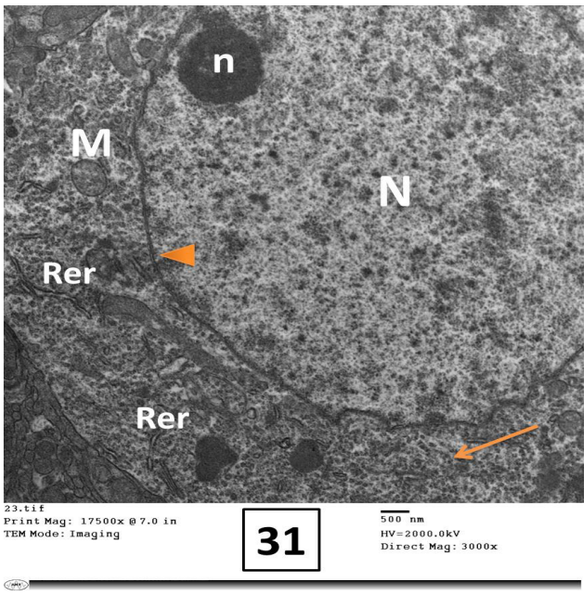


**Fig. 31:** An electron micrograph from D-gal + FSO group (IV) showing Purkinje cell with euchromatic nucleus (N) and prominent nucleolus (n). The nuclear membrane appeared double walled (arrowhead). The cytoplasm contains mitochondria (M) with regular intact cristae, cisternae of rough endoplasmic reticulum (Rer) and free ribosomes (orange arrow). (TEM × 3000)

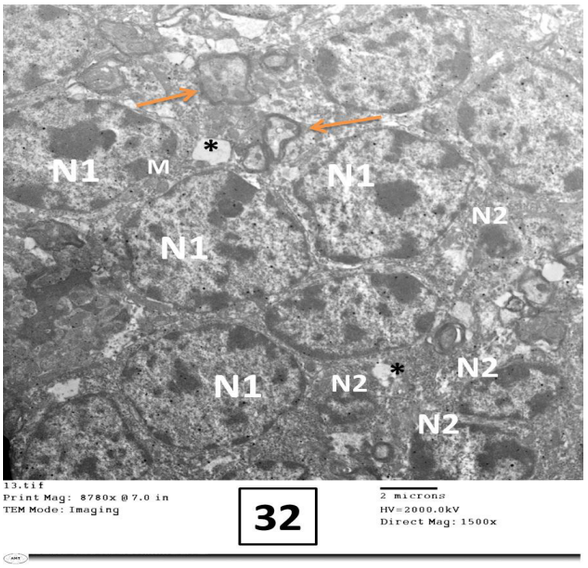


**Fig. 32:** An electron micrograph from D-gal + FSO group (IV) showing most of granule cells appear normal with heterochromatic nucleus (N1) and surrounded by thin rim of cytoplasm containing mitochondria (M). Few granule cells have shrunken and irregular nuclei (N2) with more condensed chromatin. Most nearby myelinated nerve fibers appear with normal structure (arrows), but few appear with thinning of their myelin sheath and rarefaction of their axoplasm (*). (TEM × 1500)

**Table 1:** The biochemical and statistical results in the control and experimental groups

| | Group I | Group II | Group III | Group IV | *P.value* |
|---|---|---|---|---|---|
| Serum MDA level (nmol/ml) Mean ± SD | 3.49±0.33 | 3.32±0.28 | 13.41±1.71 | 4.98±0.89 | (P1>0.05) * (P2<0.001) *** (P3<0.05) ** (P4<0.001) *** |
| Serum SOD leve (U/ml) Mean ± SD | 30.25±1.76 | 31.13±1.97 | 18.56±1.18 | 27.31±1.40 | (P1>0.05) * (P2<0.001) *** (P3<0.05) ** (P4<0.001) *** |

*P*1: Group I V Group II Non-significant * (*P*> 0.05) *P*2: Group I V Group III Significant** (*P*<0.05) *P*3: Group I V Group IV Highly significant*** (*P*<0.001) *P*4: Group III V Group IV

**Table 2:** The morphometric and statistical results in the control and experimental groups

| | Group I | Group II | Group III | Group IV | *P.value* |
|---|---|---|---|---|---|
| Number of purkinje cells Mean ± SD | 14.712.06± | 15.282.14± | 9.863.67± | 13.432.23± | (P1>0.05) * (P2<0.05) ** (P3>0.05) * (P4<0.05) ** |
| Thickness of granular layer (µm) Mean ± SD | 256.64±12.89 | 255.76±11.74 | 208.94±10.92 | 247.82±10.60 | (P1>0.05) * (P2<0.001) *** (P3>0.05) * (P4<0.001) *** |
| Area percentage of GFAP immunoexpression Mean ± SD | 8.07±0.75 | 8.53±0.67 | 36.26±4.35 | 13.21±1.47 | (P1>0.05) * (P2<0.001) *** (P3<0.05) ** (P4<0.001) *** |
| Area percentage of Caspase-3 immunoexpression Mean ± SD | 0.90±0.83 | 0.76±0.71 | 53.47±10.01 | 18.07±4.27 | (P1>0.05) * (P2<0.001) *** (P3<0.001) *** (P4<0.001) *** |
| Area percentage of calbindin immunoexpression Mean ± SD | 37.02±3.89 | 36.73±3.21 | 1.79±0.49 | 16.91±2.24 | (P1>0.05) * (P2<0.001) *** (P3<0.001) *** (P4<0.001) *** |

*P*1: Group I V Group II Non-significant * (*P*> 0.05) *P*2: Group I V Group III Significant** (*P*<0.05) *P*3: Group I V Group IV Highly significant*** (*P*<0.001) *P*4: Group III V Group IV

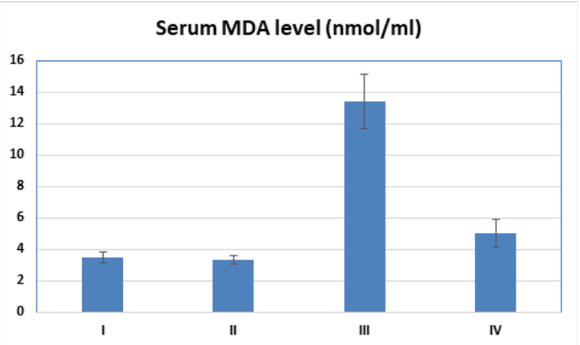


**Histogram 1:** The mean serum MDA level in the control and experimental groups

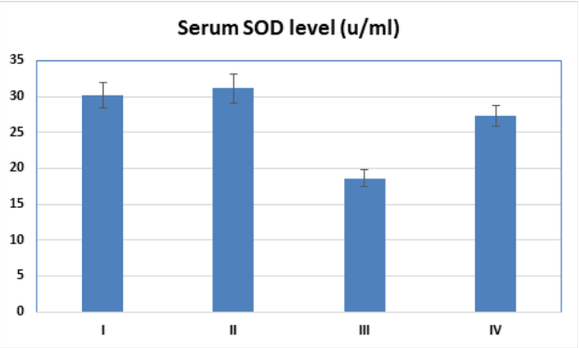


**Histogram 2:** The mean serum SOD level in the control and experimental groups

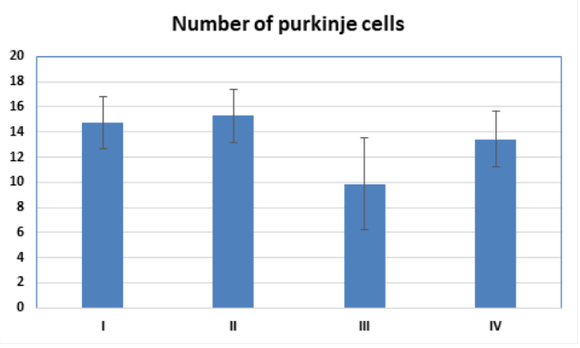


**Histogram 3:** The mean number of purkinje cells in the control and experimental groups

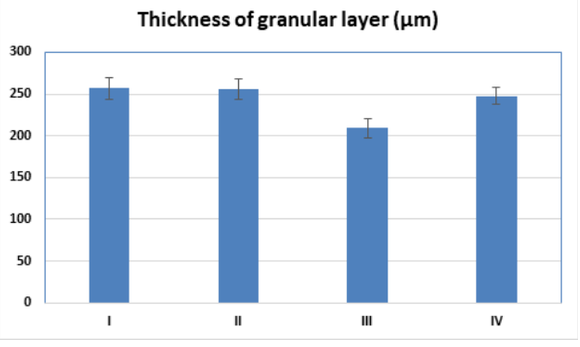


**Histogram 4:** The mean thickness of granular layer in the control and experimental groups

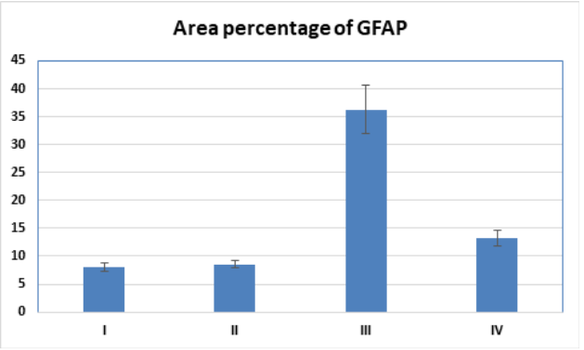


**Histogram 5:** The mean area percentage of GFAP in the control and experimental groups

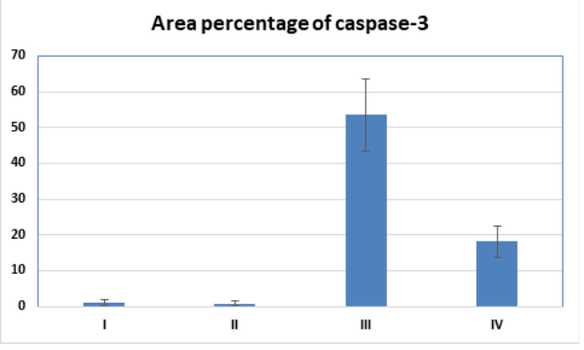


**Histogram 6:** The mean area percentage of caspase-3 in the control and experimental groups

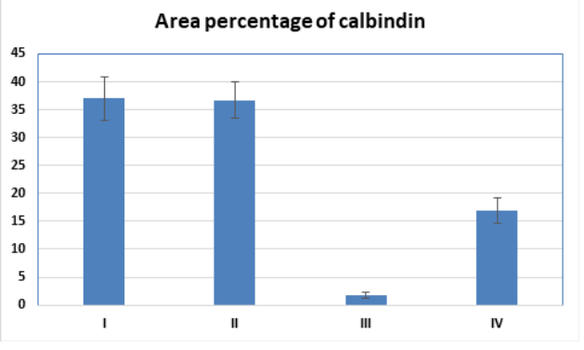


**Histogram 7:** The mean area percentage of calbindin in the control and experimental groups

## DISCUSSION

Aging is a gradual process that affects many parts of body, but brain is the organ that is most affected by aging with changes in structure and function[7, 22]. Memory loss and cognitive disorders are often caused by aging, which is a significant contributor to brain decline. Recently, the search for antiaging potent agents has become popular[2]. So, it was crucial to locate a natural agent that possesses a potential protective role against the changes induced by aging in the cerebellar cortex. Flaxseed oil was selected as the natural protective product for this study. In this study,

we used a well-established rat model of aging triggered by D-gal to determine the possible protective impact of FSO on rat cerebellar cortex in this model.

Long-term administration of D-galactose has been known to trigger oxidative stress that can imitate aging properties[6]. When D-galactose increases in the body, it can react with amino acids in peptides and proteins to form advanced glycation end products (AGEs). These products then combine with particular receptors (RAGE) in various cells, causing the nuclear factor kappa-B (NF-κB) and other signaling pathways to become activated. This leads to the release of ROS, which can accelerate the aging process. The increased level of ROS and reactive nitrogen species cause damage to proteins, lipids, and DNA, increasing the risk of various diseases including aging, neurodegenerative disorders, tumors and inflammation[3].

Typically, there is a delicate equilibrium between the production of ROS and their elimination by the antioxidant defense system. Nevertheless, when there is an overproduction of ROS and reduction in the antioxidant enzymes' activity in the brain, it leads to damage in tissue[23]. Reactive oxygen spices (ROS) have harmful impacts on human health, such as enzyme deactivation, peroxidizing membrane lipid, breaking down DNA, and triggering apoptosis[24]. MDA is recog-nized as the most crucial product of membrane lipid peroxidation triggered by increased ROS. SOD, CAT and GSH-Px are potent antioxidant enzymes which prevent free radicals creation. They are recognized as primary defense against ROS generated in times of oxidative stress[25]. The MDA, GSH and SOD levels are regarded as markers for assessing the status of oxidative stress[24].

In the current work, there were highly significant rise in MDA serum level and highly significant decline in SOD serum level of D-gal treated rats and this confirmed the oxidative stress status induced by D-gal. Such results were consistent with the results of prior studies[4,9,25] on D-galactose-induced aging. Shwe *et al*.[26] stated that high levels of D-gal result in its oxidation by galactose oxidase, producing $H_2O_2$ (hydrogen peroxide). This leads to a reduction in SOD levels. The increased H2O2 then reacts with reduced iron to generate hydroxide ions (OH−). Both $H_2O_2$ and OH− are reactive oxygen species that can trigger lipid peroxidation in cell membrane and disrupt redox balance, ultimately causing neuronal damage. They added that a decline in the antioxidant enzymes like SOD, GSH-Px and CAT by D-galactose causes an imbalance between antioxidant activities and reactive oxygen species and hence increases oxidative stress and mitochondria dysfunction.

The histological and immunohistochemical results of D-gal treated rats (group III) in the current study confirmed the neuronal damage associated with oxidative stress of D-galactose-induced aging. There were shrunken irregular Purkinje cells with pyknotic nuclei, Purkinje cell loss with empty spaces, Purkinje cells organized in several layers, deeply stained and clumped granule cells with wide spaces in between, mitochondria with destroyed cristae, apparent decrease in the granular layer thickness. Also, there were vacuolated neuropil, irregularly dilated myelinated axons with reduced myelin thickness and rarefaction of their axoplasm and dilated congested blood vessels. Such results were supported by the statistical results in this study as there was significant decrease in Purkinje cell number and thickness of granular layer. These histological results were in line with the results of earlier studies[25,3,6] on D-galactose-induced brain aging in which the researchers detected Pyknosis, necrosis and loss of neurons of the cerebellar cortex.

In this study, the presence of pyknotic nuclei may reflect an apoptotic state as previously reported [27]. Also, vacuolated neuropil observed in the H&E-stained sections of D-gal group could be explained by cell shrinkage and loss of cellular processes[27]. Electron microscopic result of this group supported such explanation as there were irregularly dilated myelinated axons and their myelin became thinner and their axoplasm exhibited rarefaction.

The arrangement of Purkinje cells in multiple layers could be explained by Purkinje cells attempt to fulfill their function by being crowded in multiple layers to reestablish synaptic connection with other nerve cells[28].

In the current study, the staining for Nissl's granules in Purkinje and granule cells of D-gal group (III) showed a reduction in intensity. Such result was in line with prior work[29] where the authors detected a reduction in number of Nissl granules in the hippocampus neurons by D-gal.

In the present study, the immunohistochemical results supported the observed histological results. GFAP stained sections of D-gal treated rats (group III) exhibited strong GFAP immunoreaction in many astrocytes dispersed in cerebellar cortex. This was confirmed statistically by highly significant rise in GFAP immunoreaction relative to control. Similar finding was reported in a previous research[30] in which the authors detected elevated GFAP expression with increased astrocyte number in all brain regions as a result of D-galactose-induced oxidative stress. This positive reaction could be explained by astrogliosis which is defined as astrocytes proliferation and enlargement with increased expression of GFAP as a result of any chemical, degenerative or mechanical injury to brain[31].

Elevated levels of ROS can potentially activate Caspase-3, a significant factor in apoptosis, leading to neuronal damage[32]. This was in harmony with the present study as caspase-3 exhibited strong positive immunoreaction in cerebellar cortex of D-gal treated rats (group III). Statistical analysis confirmed that by a highly significant rise of caspase-3 immunoreaction compared to control. Such finding was reported in a previous study[33] in which the authors stated that oxidative stress and inflammation induced by D-gal are two mechanisms working in harmony to trigger apoptosis in the cells.

Calcium plays an important role as an intracellular signaling molecule controlling many cell activities, but it is involved in the neurodegenerative process. Several pathways of cell damage share to cause marked rise in intracellular calcium level, triggering a sequence of caspases and initiating apoptosis. Therefore, it is crucial for neurons to maintain calcium homeostasis for their well-being. The function of calcium essentially relies on a set of proteins, called calcium-binding proteins, which are expressed by neurons. Calbindin is a protein that binds to calcium and safeguards neurons from harm resulting from excessive levels of calcium. It is present in neurons within the nervous system. Calbindin plays a potent role in maintaining calcium balance, protecting cells from programmed cell death, and impeding the degeneration of neurons[34,3]. To clarify this point, calbindin immunoreaction was estimated in the current work and D-gal was found to induce highly significant decrease in area percent of calbindin immunoreaction in the cerebellar cortex resulting in activated caspase 3 that triggered cell apoptosis. Such result was in line with previous study[3].

In group IV, flaxseed oil was given with D-galactose to assess its possible role in alleviating the aging influence on the cerebellar cortex. Flaxseed oil exerted a protective effect on cerebellar cortex as shown by the histological and immunohistochemical findings. The results exhibited much preservation of the histological structure of the cerebellar cortex. The molecular, Purkinje cell and granular layers had normal appearance except for few changes. There were few Purkinje cells with pyknotic nuclei, few granule cells with shrunken irregular nuclei and few myelinated nerve fibers displaying splitting with loss of compact lamellar structure. Morphometric and statistical results of this group confirmed such findings. These findings matched with a previous work[35] in which the authors detected reduced hippocampal neuronal loss by flaxseed oil in their study on induced neurodegeneration.

The protective role of flaxseed oil owed to its antioxidant and anti-inflammatory characteristics as has been reported by Ismail *et al*.[12] who stated that FSO has a neuroprotective role on CCl4-induced brain damage by scavenging free radicals, enhancing the antioxidant enzymes, increasing GSH level and reducing inflammatory response. Biochemical results of group IV (D-gal + FSO) confirmed such explanation as there were drop in serum MDA level and an increase in serum SOD level compared to group III (D-gal). Similar outcomes were obtained by Tashkandi *et al*.[13] in their study on protective impact of FSO on nephrotoxicity. They attributed antioxidant capabilities of FSO to its rich content of omega-3 fatty acids which act as free radicals scavengers. As a result, the activity of the SOD and GSH enzymes was enhanced. According to Mishra *et al*.[36], the neuroprotective effect of FSO was owed to omega 3 fatty acids which play a defensive role in the brain against peroxidation by the mechanism of adaptable fluidity of cell membrane and its enzymes. Moreover, Badawy *et al*.[11] suggested that omega-3 PUFAs in FSO may have alleviating effect on brain damage by two potential ways. Firstly, they may boost catalase levels in the peroxisome and cytoplasm, improving defense against free oxygen radicals. Secondarily, Omega-3 polyunsaturated fatty acids in FSO may replace the polyunsaturated fatty acid components of the membranes that have been damaged by ROS.

Kassab[37] attributed the anti-inflammatory action of flaxseed to omega-3 fatty acids which reduce the release of the inflammatory cytokines as IL-1, IL-6, TNF and CRP by inhibiting NF-Kb. The author added that Omega-3 fatty acids control the expression of adhesion molecules like VCAM-1, which aids in leukocyte endothelial interaction.

Moreover, the neuroprotective effect of FSO could be attributed to Omega-3 polyunsaturated fatty acids that have been shown to promote neurogenesis in a variety of animal studies as previously reported[38]. To clarify this point, Medoro *et al*.,[39] reported that decreased adult neurogenesis, or the gradual depletion of neural stem cells in adult neurogenic niches, is considered a hallmark of brain aging. They added that many factors regulate neurogenesis in adult brain, which has an effect on neural stem cells differentiation and fate. These elements comprise both extrinsic and intrinsic components, as hormones, growth factors, neurotrophins, inflammatory cytokines, physical exercise, and diet. Many dietary bioactive substances have been proven to control and promote neurogenesis in adult progenitor cells. Dyall *et al*.[40] stated that dietary supplementation with the omega-3 PUFAs could increase neurogenesis in aged rats and this contributes to its neuroprotective effects in brain aging. Purkinje cells could be regenerated via Bone marrow-derived cells that cross the blood brain barrier and fuse with Purkinje cells in the cerebellum giving them their nuclear genetic material[41]. On the other hand, the granule cells could be regenerated from external granular layer that contains granule cell progenitors that will differentiate and then migrate into the cerebellum[42].

As regard group IV, GFAP immunoreaction exhibited significant reduction relative to group III. Such finding agreed with an earlier research[35] in which the authors detected attenuated GFAP expression by FSO treatment suggesting that FSO can decrease pro-inflammatory cytokines and astrocyte stimulation.

Caspase-3 immunoreaction of group IV revealed significant reduction relative to group III reflecting the anti-apoptotic role of FSO. Similar result was obtained by Mitrović *et al*.[35] who reported that FSO administration reduced the hippocampal cell damage, likely by inhibiting the caspase-3 signaling pathway, decreasing the presence of the pro-apoptotic factor Bax, and rising Bcl-2 reaction. These findings suggest that FSO protected the structure and function of mitochondria. Moreover, Kassab[37] attributed anti-apoptotic effect of flaxseed to its main component α-linolenic acid which hinders both extrinsic and intrinsic cell death pathways that are activated by

prolonged stimulation of inflammatory cytokines. It also stops cytochrome-c release and keeps the mitochondria's outer membrane from depolarization caused by cytokines.

## CONCLUSION

These findings provided evidence that D-gal can create aging process in rats manifested by biochemical abnormality, histological and immunohistochemical alterations in the cerebellar cortex. FSO was able to minimize D-gal-induced changes. These findings suggest that FSO can provide neuroprotective impact in the aging process through its antioxidant and anti-inflammatory properties. So, FSO may be promising approach in the prevention of aging-relative disorders.

## CONFLICT OF INTERESTS

There are no conflicts of interest

## REFERENCES


1. Li H, Zheng L, Chen C, Liu X and Zhang W. Brain Senescence Caused by Elevated Levels of Reactive Metabolite Methylglyoxal on D-Galactose-Induced Aging Mice. Front. Neurosci. 2019; 13:1004. doi: 10.3389/fnins.2019.01004
2. Sun K, Yang P, Zhao R, Bai Y and Guo Z. Matrine Attenuates D-Galactose-Induced Aging-Related Behavior in Mice via Inhibition of Cellular Senescence and Oxidative Stress. Oxidative Medicine and Cellular Longevity, 2018; 2018: 12. https://doi.org/10.1155/2018/7108604
3. El-Far AH, Elewa YHA, Abdelfattah EA, Alsenosy AA, Atta MS, Abou-Zeid KM, Al Jaouni SK, Mousa SA and Noreldin AE. Thymoquinone and Curcumin Defeat Aging-Associated Oxidative Alterations Induced by D-Galactose in Rats' Brain and Heart. Int J Mol Sci. 2021; 22(13):6839. doi: 10.3390/ijms22136839.
4. Fatemi I, Khaluoi A, Kaeidi A, Shamsizadeh A, Heydari S and Allahtavakoli M. Protective effect of metformin on D-galactose-induced aging model in mice. Iran J Basic Med Sci. 2018; 21:19-25. doi: 10.22038/IJBMS.2017.24331.6071
5. Azman KF and Zakaria R. D-Galactose-induced accelerated aging model: an overview. Biogerontology, 2019; 20: 763–782. https://doi.org/10.1007/s10522-019-09837-y
6. HEJAZ S. Study of cerebellar tissue following induction of aging in mice by Di-galactose. Int. J. Morphol. 2023; 41(3): 825-830. http://dx.doi.org/10.4067/S0717-95022023000300825.
7. Lee J, Kim YS, Kim E, Kim Y, Kim Y. Curcumin and hesperetin attenuate D-galactose-induced brain senescence in *vitro* and in *vivo*. Nutr Res Pract. 2020; 14(5): 438-452. doi: 0.4162/nrp.2020.14.5.438.
8. Hou Y, Dan X, Babbar M, Wei Y, Hasselbalch SG, Croteau DL and Bohr VA. Ageing as a risk factor for neurodegenerative disease. Nat Rev Neurol. 2019; 15(10): 565-581. doi: 10.1038/s41582-019-0244-7.
9. Kim Y and Kim Y. L-histidine and L-carnosine exert anti-brain aging effects in D-galactose-induced aged neuronal cells. Nutr Res Pract. 2020; 14(3): 188-202. doi: 10.4162/nrp.2020.14.3.188.
10. Rudolph S, Badura A, Lutzu S, Pathak SS, Thieme A, Verpeut JL, Wagner MJ, Yang Y and Fioravante D. Cognitive-Affective Functions of the Cerebellum. The Journal of Neuroscience, 2023; 43(45):7554–7564. DOI: https://doi.org/10.1523/JNEUROSCI.1451-23.2023.
11. Badawy EA, Rasheed WI, Elias TR, Hussein J, Harvi M, Morsy S and Mahmoud Y. Flaxseed oil reduces oxidative stress and enhances brain monoamines release in streptozotocin-induced diabetic rats. Hum Exp Toxicol. 2015; 34(11):1133-8. doi: 10.1177/0960327115571765.
12. Ismail AF, Salem AA, Eassawy MM. Modulation of gamma-irradiation and carbon tetrachloride induced oxidative stress in the brain of female rats by flaxseed oil. J Photochem Photobiol B. 2016; 161:91-9. doi: 10.1016/j.jphotobiol.2016.04.031.
13. Tashkandi1 B, Baghdadi GM and Baghdadi AM. Protective Impact of Flaxseed Oil against Acetaminophen-Induced Nephrotoxicity in Rats: Antioxidant and Anti-inflammatory Pathway. Journal of Complementary Medicine Research, 2023; 14 (1): 56-60. DOI: 10.5455/jcmr.2023.14.01.11
14. El Makawy A, Eissa F, EL-Bamby M and Elhamalawy O. "Flaxseed oil as a protective agent against bisphenol-A deleterious effects in male mice. Bulletin of the National Research Centre, 2018; 42 (1): 1-9. DOI: 10.1186/s42269-018-0007-4
15. Denis I, Potier B, Heberden C and Vancassel S. Omega-3 polyunsaturated fatty acids and brain aging. Curr Opin Clin Nutr Metab Care. 2015; 18(2):139-46. doi: 10.1097/MCO.0000000000000141.
16. Gaertner, DJ, Hallman, TM, Hankenson, FC and Batchelder, MA. Anesthesia and analgesia for laboratory rodents. In: Fish, R.E., Danneman, P.J., Brown, M., Karas, A.Z. (Eds.), Anesthesia and Analgesia in Laboratory Animals. , 2nd ed. Academic Press, London (UK), 2008; 239–297. Hardback ISBN: 9780123738981. eBook ISBN: 9780080559834.
17. Kiernan JA: Histological and histochemical methods; theory and practice. 5th ed Oxford, UK: Butterworth Heinemann, (2015); 238–310. ISBN 9781907904325
18. Gokul S and Akhil A. (2012): "Toluidine blue: A review of its chemistry and clinical utility". J oral Maxillofac Pathol. 2012; 16(2): 251-255. Doi: 10.4103/0973-029x.99081

19. Suvarna SK, Layton C and Bancroft JD: Immunohistochemical techniques. In: Bancroft's Theory and Practice of Histological Techniques, 7th ed., Churchill Livingstone Elsevier, London. 2013; pp: 387-418. ISBN: 978-0-7020-4226-3

20. Suvarna SK, Layton C and Bancroft JD: Transmission electron microscopy. In: Bancroft's Theory and Practice of Histological Techniques, 7th ed., Elsevier Churchill Livingstone, London. 2013; pp: 493-508. ISBN: 978-0-7020-4226-3

21. Emsley R, Dunn G and White IR. Mediation and moderation of treatment effects in randomized controlled trials of complex interventions. Stat Methods Med Res. 2010; 19: 237-270. doi: 10.1177/096228020

22. Safdar A, Azman K, Zakaria R, Ab Aziz C B and Rashid U. Memory-enhancing effects of goat milk in D-galactose-induced aging rat model. Biomedical Research and Therapy, 2020; 7(1): 3563-3571. DOI : 10.15419/bmrat.v7i1.583

23. Zhang Y, Liu B, Chen X, Zhang N, Li G, Zhang L-H and Tan L-Y. Naringenin ameliorates behavioral dysfunction and neurological deficits in a D-galactose-induced aging mouse model through activation of PI3K/Akt/Nrf2 pathway. Rejuvenation Res. 2017; 20: 462–472. doi: 10.1089/rej.2017.1960.

24. Zhen YZ, Lin YJ, Li KJ, Zhang GL, Zhao YF, Wang MM, Wei JB, Wei J and Hu G. Effects of rhein lysinate on D-galactose-induced aging mice. Exp Ther Med. 2016; 11(1): 303-308. doi: 10.3892/etm.2015.2858.

25. Liu H , Zhang X , Xiao J , Song M , Cao Y , Xiao H , Liu X . Astaxanthin attenuates d-galactose-induced brain aging in rats by ameliorating oxidative stress, mitochondrial dysfunction, and regulating metabolic markers. Food Funct. 2020; 11(5): 4103-4113. doi: 10.1039/d0fo00633e.

26. Shwe T, Pratchayasakul W, Chattipakorn N and Chattipakorn SC. Role of D-galactose-induced brain aging and its potential used for therapeutic interventions. Exp Gerontol. 2018; 101: 13-36. doi: 10.1016/j.exger.2017.10.029.

27. Abdel Mohsen AF, Ahmed NA, Altiab ZM and Zaher SM. Effect of Cisplatin on Cerebellar Cortex of Albino Rat and Possible Protective Role of Granulocyte Colony Stimulating Factor versus Citrullus Lanatus Juice: A Histological Study. EJH. 2019; 43(3): 702-717. DOI: 10.21608/ejh.2019.19193.1197

28. Laag EM and Tawfik SM. Histological Study of the Possible Protective Action of Platelet Rich Plasma on the Injurious Effect Induced by Aluminum Chloride on Albino Male Rat Cerebellar Cortex. EJH. 2021; 44(4):1107-1117. DOI: 10.21608/ejh.2021.49889.1386

29. Li P, Ma Y, Wang X, Li X, Wang X, Yang J and Liu G. The protective effect of PL 1-3 on D-galactose-induced aging mice. Front. Pharmacol. 2024; 14: 1304801. doi: 10.3389/fphar.2023.1304801

30. Saafan SM, Mohamed SA, Noreldin AE, *et al*. Rutin attenuates D-galactose-induced oxidative stress in rats' brain and liver: molecular docking and experimental approaches. Food & Function. 2023; 14(12): 5728-5751. DOI: 10.1039/d2fo03301a.

31. Abd El-Wahed NAA, Geith EZ, Kalleny NK and Abd Al-Khalek HA. (2019):" The Effect of Diet Coke and Monosodium Glutamate on the Cerebellar Cortex of Adult Male Albino Rats. Histological and Immuno-histochemical Study". EJH. 2019; 42 (2): 437-452. DOI: 10.21608/EJH.2019.7279.1071

32. Xu L-Q, Xie Y-L, Gui S-H, Zhang X, Mo Z-Z, Sun C-Y, Li C-L, Luo D-D, Zhang Z-B, Su Z-R. Polydatin attenuates D-galactose-induced liver and brain damage through its anti-oxidative, anti-inflammatory and anti-apoptotic effects in mice. Food Funct. 2016; 7: 4545–4555. doi: 10.1039/C6FO01057A.

33. Atef MM, Emam MN, Abo El Gheit RE, Elbeltagi EM, Alshenawy HA, Radwan DA, Younis RL and Abd-Ellatif RN. Mechanistic Insights into Ameliorating Effect of Geraniol on D-Galactose Induced Memory Impairment in Rats. Neurochem Res. 2022; 47(6): 1664-1678. doi: 10.1007/s11064-022-03559-3.

34. Ouh IO, Kim YM, Gim SA and Koh PO. Focal cerebral ischemic injury decreases calbindin expression in brain tissue and HT22 cells. Lab Anim Res. 2013; 29(3):156-61. doi: 10.5625/lar.2013.29.3.156.

35. Mitrović N, Dragić M, Zarić M, Nedeljković N and Grković I. Flaxseed Oil Attenuates Trimethyltin-induced Neurodegeneration via Down-regulation of Inflammatory Activity of Astrocytes. Research Square, 2021. DOI: 10.21203/rs.3.rs-277617/v1

36. Mishra DK, Srivast D, Fatima Z, Mohapatra L and Awasthi H. Neuroprotective Potential of Flaxseed Oil in Amelioration of Cadmium Induced Neurotoxicity. Research Square; 2022. DOI: 10.21203/rs.3.rs-1694868/v1.

37. Kassab AA. The potential protective role of flaxseed extract on ventral prostate in a rat model of streptozotocin-induced diabetes: A histological and immunohistochemical study. EJH. 2019; 42(2): 425-436. DOI: 10.21608/ejh.2019.6454.1047

38. Dyall SC. The role of omega-3 fatty acids in adult hippocampal neurogenesis. OCL. 2011; 18(5): 242-245. doi : 10.1684/ ocl.2011.0392

39. Medoro A, Davinelli S, Milella L, Willcox BJ, Allsopp RC, Scapagnini G and Willcox DC. Dietary Astaxanthin: A Promising Antioxidant and Anti-Inflammatory Agent for Brain Aging and Adult Neurogenesis. Marine Drugs. 2023; 21(12):643. https://doi.org/10.3390/md21120643

40. Dyall SC, Michael GJ and Michael-Titus AT. Omega-3 fatty acids reverse age-related decreases in nuclear receptors and increase neurogenesis in old rats. J Neurosci Res. 2010; 88(10):2091-102. doi: 10.1002/jnr.22390. PMID: 20336774.

41. Kemp K, Wilkins A and Scolding N. Cell fusion in the brain: two cells forward, one cell back. Acta Neuropathol. 2014; 128:629–638. DOI 10.1007/s00401-014-1303-1

42. Lackey EP, Heck DH and Sillitoe RV. Recent advances in understanding the mechanisms of cerebellar granule cell development and function and their contribution to behavior. F1000Res. 2018; 7:F1000 Faculty Rev-1142. doi: 10.12688/f1000research.15021.1. PMID: 30109024; PMCID: PMC6069759.

**الملخص العربى**

# الدور الوقائي المحتمل لزيت بذرة الكتان على قشرة المخيخ في نموذج الشيخوخة المستحث بالدي جالاكتوز في الجرذ: دراسة هستولوجية و هستوكيميائية مناعية

**داليا السيد الغزولي**

**قسم الهستولوجي- كلية الطب- جامعة المنوفية**

**الخلفية:** الشيخوخة عملية طبيعية تؤثر على أعضاء الجسم المختلفة. عادةً ما يتم إنشاء نماذج الشيخوخة في الحيوانات باستخدام الدي جالاكتوز. زيت بذرة الكتان هو مكمل غذائي مليء بأحماض أوميجا ٣ الدهنية المتعددة غير المشبعة التي لها العديد من الفوائد الصحية.

**الهدف:** كان الهدف من هذا العمل هو استكشاف التأثير الوقائي المحتمل لزيت بذرة الكتان على قشرة المخيخ في نموذج الشيخوخة المستحث بالدي جالاكتوز في الجرذ.

**مواد و طرق البحث:** تم تصنيف أربعين من ذكور الجرذان البيضاء البالغة بالتساوي إلى أربع مجموعات: المجموعة الأولى (المجموعة الضابطة)، المجموعة الثانية (المجموعة المعالجة بزيت بذرة الكتان): تلقت زيت بذرة الكتان ١,٢ مل/ كجم/ يوم، المجموعة الثالثة (المجموعة المعالجة بالدي جالاكتوز): تلقت دي جالاكتوز ٢٠٠ ملجم / كجم / يوم، المجموعة الرابعة (المجموعة المعالجة بالدي جالاكتوز و زيت بذرة الكتان): تلقت زيت بذرة الكتان و دي جالاكتوز باستخدام جرعات مماثلة للمجموعات السابقة. لمدة ستة أسابيع، تم إعطاء الدواء مرة واحدة يوميا. في نهاية هذه التجربة، تم جمع عينات المخيخ وإخضاعها للفحص بالمجهر الضوئي والإلكتروني. تم عمل دراسات مورفومترية وإحصائية.

**النتائج:** كشفت المجموعة المعالجة بالدي جالاكتوز عن تغيرات حادة في قشرة المخيخ. أظهرت الطبقة الجزيئية انوية داكنة و تفريغ في المنطقة المحيطة بالخلايا. بدت خلايا بركنجي منكمشة وغير منتظمة الشكل مع نواة متغايرة اللون منكمشة و اتساع فى الشبكة الإندوبلازمية الخشنة. كما فُقدت العديد من خلايا بركنجي وتركت مساحات فارغة. ظهرت الخلايا الحبيبية منكمشة و داكنة ومتكتلة في مجموعات. كما لوحظ وجود ارتفاع ذو دلالة إحصائيه كبيرة في التفاعل المناعي للبروتين الليفي الحامضي ولكاسبس-٣ وانخفاض ذو دلالة إحصائيه كبيرة في التفاعل المناعي للكالبيندين مقارنة بالمجموعة الضابطة. تم اكتشاف تغيرات ذو دلالة إحصائيه كبيرة في مستويات المالونديالدهيد وسوبر أكسيد ديسميوتاز في الدم مقارنة بالمجموعة الضابطة. إعطاء زيت بذرة الكتان مع دي جالاكتوز قلل من هذه التغيرات.

**الخلاصة:** يستطيع زيت بذرة الكتان أن يوفر تأثيرًا وقائيًا للأعصاب في عملية الشيخوخة من خلال تأثيراته المضادة للأكسدة والمضادة للالتهاب.